Static structure of polydisperse colloidal monolayers

F. Lado[a)]
Instituto de Química Física Rocasolano, CSIC, Serrano 119, E-28006 Madrid, Spain

(Received 8 December 1997; accepted 15 January 1998)

A generalization of integral equation theory of simple liquids is used to study the structure and thermodynamics of a monolayer of spherical colloidal particles having a continuous distribution $f(\sigma)$ of diameters σ. The quasi-two-dimensional fluid is modeled using both a repulsive Yukawa potential to represent charged hard spheres (with attendant charge polydispersity) and a Lennard-Jones potential to represent soft spheres with an effective attractive well. The numerical solution of the integral equations makes essential use of polynomials that are orthogonal with weight function $f(\sigma)$, which is taken here to be a Schulz distribution. © *1998 American Institute of Physics.* [S0021-9606(98)51715-1]

I. INTRODUCTION

Colloidal particles, at the boundary of the microscopic and macroscopic worlds, provided the first direct evidence for the atomic hypothesis through Einstein's 1905 explanation of Brownian motion and thereby gave credibility to the new techniques of statistical mechanics then being applied to the hypothetical atoms. It seems fitting that nearly a century later colloidal suspensions should also offer a visible model for the application of the most elementary statistical technique of all, namely *counting*, to determine a fluid structure akin to that of atoms. *Digital video microscopy*[1] makes possible the direct measurement of the averaged structure of a colloidal fluid,[2–6] a sort of real-world ''molecular dynamics simulation.'' For suspensions narrowly confined between parallel glass plates, the particles form a quasi-two-dimensional fluid. The direct measurement of the structure of a monolayer of charged polystyrene spheres of micrometer scale in a confined aqueous solution can then be made to yield an effective pair potential. Kepler and Fraden[5] and Carbajal *et al.*[6] found in this way a potential that is short ranged with a significant attractive component, in contrast to the essentially repulsive interaction between unconfined charged colloidal spheres, while Crocker and Grier[4] determined a repulsive interaction with a notably smaller Debye-Hückel screening length than that of an unconfined suspension. From the theoretical side, two-dimensional models of colloidal fluids with repulsive potentials have been studied using both simulation[7–9] and integral equations.[9–11]

All of these calculations have been for monodisperse colloidal suspensions. In this paper, we use integral equations to study the effects of size and charge polydispersity on two-dimensional fluids. The effective potential that arises in confined suspensions being still uncertain, we use two familiar interaction models: (a) the repulsive part of the Derjaguin-Landau-Verwey-Overbeek (DLVO) interaction[12–14] and (b) the Lennard-Jones 12-6 interaction.[15]

[a)]On sabbatical leave from Department of Physics, North Carolina State University, Raleigh, North Carolina 27695-8202.

II. INTEGRAL EQUATION FORMALISM FOR A MONOLAYER OF POLYDISPERSE SPHERES

We consider a uniform monolayer of N polydisperse colloidal spheres occupying a plane area A at temperature T. The density of particles at point $\mathbf{r}$ with diameter σ is given by the one-body density function

$$\rho^{(1)}(\mathbf{r},\sigma)=\left\langle \sum_{i=1}^{N} \delta(\mathbf{r}-\mathbf{r}_i)\,\delta(\sigma-\sigma_i)\right\rangle=\rho f(\sigma), \tag{1}$$

where $\rho=N/A$ and $f(\sigma)$ is the fixed distribution of particle diameters σ. The two-body density function

$$\begin{aligned}\rho^{(2)}&(\mathbf{r},\sigma,\mathbf{r}',\sigma')\\ &=\left\langle \sum_{i\neq j} \delta(\mathbf{r}-\mathbf{r}_i)\,\delta(\sigma-\sigma_i)\,\delta(\mathbf{r}'-\mathbf{r}_j)\,\delta(\sigma'-\sigma_j)\right\rangle\\ &=\rho^2 f(\sigma) f(\sigma') g(|\mathbf{r}-\mathbf{r}'|,\sigma,\sigma')\end{aligned} \tag{2}$$

then defines the generalized pair distribution function $g(r,\sigma,\sigma')$, which is the key quantity needed for a complete description of the structure and thermodynamics of the colloidal monolayer. In these expressions, $\mathbf{r}_i$ is the location of particle i in the plane and σ_i its diameter; the angular brackets denote a canonical ensemble average.

In classical liquid state theory, the pair distribution function is obtained from the Ornstein-Zernike (OZ) equation combined with a closure relation.[15] The first of these, generalized for polydispersity, reads

$$\begin{aligned}\gamma(r_{12},\sigma_1,\sigma_2)=\rho\int d\mathbf{r}_3 d\sigma_3 f(\sigma_3)[c(r_{13},\sigma_1,\sigma_3)\\ +\gamma(r_{13},\sigma_1,\sigma_3)]c(r_{32},\sigma_3,\sigma_2)\end{aligned} \tag{3}$$

for the indirect correlation function $\gamma=g-1-c$, where c is the direct correlation function. The second, or closure, relation expresses c back in terms of γ and the pair interaction ϕ,

$$\begin{aligned}c(r,\sigma_1,\sigma_2)=\exp[-\beta\phi(r,\sigma_1,\sigma_2)+\gamma(r,\sigma_1,\sigma_2)\\ +b(r,\sigma_1,\sigma_2)]-1-\gamma(r,\sigma_1,\sigma_2),\end{aligned} \tag{4}$$

where $\beta=1/k_BT$, with k_B Boltzmann's constant. This equation must be supplemented with an approximation for $b(r,\sigma_1,\sigma_2)$, the so-called bridge function, whose formal definition as an infinite series in density[15] offers only modest practical guidance. Most approximate closures for c define b implicitly.

The numerical evaluation of the OZ equation is simpler in Fourier transform representation, which deconvolutes the **r** integral. Thus, in transform space, Eq. (3) becomes

$$\tilde{\gamma}(k,\sigma_1,\sigma_2)=\rho\int_0^\infty d\sigma_3 f(\sigma_3)[\tilde{c}(k,\sigma_1,\sigma_3) + \tilde{\gamma}(k,\sigma_1,\sigma_3)]\tilde{c}(k,\sigma_3,\sigma_2), \tag{5}$$

with one remaining integration. We note that the Fourier transform of a circularly symmetric function in two dimensions becomes a Hankel transform,

$$\tilde{w}(k)=2\pi\int_0^\infty dr\ rw(r)J_0(kr), \tag{6}$$

where $J_0(x)$ is the zeroth-order Bessel function; the inverse of (6) is

$$w(r)=\frac{1}{2\pi}\int_0^\infty dk\ k\tilde{w}(k)J_0(kr). \tag{7}$$

The final integration in Eq. (5) can also be eliminated and the evaluation of the OZ equation reduced to algebra by now expanding all σ-dependent functions in orthogonal polynomials $p_j(\sigma)$, $j=0,1,2,\ldots$, defined such that

$$\int_0^\infty d\sigma\ f(\sigma)p_i(\sigma)p_j(\sigma)=\delta_{ij}, \tag{8}$$

where δ_{ij} is the Kronecker delta. Then with

$$\tilde{\gamma}(k,\sigma_1,\sigma_2)=\sum_{i,j=0}^{\infty}\tilde{\gamma}_{ij}(k)p_i(\sigma_1)p_j(\sigma_2) \tag{9}$$

and a similar expansion of $\tilde{c}(k,\sigma_1,\sigma_2)$, Eq. (5) becomes

$$\tilde{\gamma}_{ij}(k)=\rho\sum_l[\tilde{c}_{il}(k)+\tilde{\gamma}_{il}(k)]\tilde{c}_{lj}(k), \tag{10}$$

or, in matrix notation,

$$\tilde{\Gamma}(k)=\rho[\tilde{C}(k)+\tilde{\Gamma}(k)]\tilde{C}(k)=\rho\tilde{C}(k)\tilde{C}(k)[I-\rho\tilde{C}(k)]^{-1}. \tag{11}$$

In these equations $\tilde{\Gamma}(k)$, $\tilde{C}(k)$ are symmetric matrices with elements $\tilde{\gamma}_{ij}(k)$, $\tilde{c}_{ij}(k)$ and I is the unit matrix. Orthonormality allows the easy inversion of Eq. (9) as

$$\tilde{\gamma}_{ij}(k)=\int d\sigma_1\ d\sigma_2\ f(\sigma_1)f(\sigma_2)\tilde{\gamma}(k,\sigma_1,\sigma_2)p_i(\sigma_1)p_j(\sigma_2). \tag{12}$$

Similar expansions and inversions hold for functions in r space.

With the substitution of the J_0 transforms (6) and (7) for the corresponding sine transforms, these ingredients for a polydisperse fluid in two dimensions are identical to those of a polydisperse fluid in three dimensions[16] and can be solved with the same numerical procedures. The new feature, the Hankel transform, is evaluated using an orthogonality-preserving algorithm.[17]

The generalized pair distribution function

$$g(r,\sigma_1,\sigma_2)=\exp[-\beta\phi(r,\sigma_1,\sigma_2) + \gamma(r,\sigma_1,\sigma_2)+b(r,\sigma_1,\sigma_2)] \tag{13}$$

is finally constructed from the self-consistent solution of the (OZ+closure) equations for the coefficients $\gamma_{ij}(r)$. The thermodynamic quantities then directly computable from g are the internal energy U,

$$\frac{\beta U}{N}=\frac{1}{2}\rho\int d\mathbf{r}\ d\sigma\ d\sigma'\ f(\sigma)f(\sigma') \times g(r,\sigma,\sigma')\beta\phi(r,\sigma,\sigma'), \tag{14}$$

and the pressure p,

$$\frac{\beta p}{\rho}=1-\frac{1}{4}\rho\int d\mathbf{r}\ d\sigma\ d\sigma'\ f(\sigma)f(\sigma') \times g(r,\sigma,\sigma')r\frac{d\beta\phi(r,\sigma,\sigma')}{dr}. \tag{15}$$

In addition, the isothermal compressibility K_T,

$$\frac{1}{\rho k_BTK_T}\equiv\beta\left(\frac{\partial p}{\partial\rho}\right)_T =1-\rho\int d\mathbf{r}\ d\sigma\ d\sigma'\ f(\sigma)f(\sigma')c(r,\sigma,\sigma') =1-\rho\tilde{c}_{00}(0), \tag{16}$$

is obtained from the direct correlation function.

Pair functions of interest can be expressed directly in terms of the computed coefficients. In particular, the number-number pair distribution function and the number-number structure factor[18] are, respectively,

$$g_{NN}(r)\equiv\int d\sigma_1\ d\sigma_2\ f(\sigma_1)f(\sigma_2)g(r,\sigma_1,\sigma_2)=g_{00}(r), \tag{17}$$

$$S_{NN}(k)\equiv\int d\sigma_1\ d\sigma_2[f(\sigma_1)\delta(\sigma_1-\sigma_2) + \rho f(\sigma_1)f(\sigma_2)\tilde{h}(k,\sigma_1,\sigma_2)]=1+\rho\tilde{h}_{00}(k). \tag{18}$$

Further, low order coefficients of $g(r,\sigma_1,\sigma_2)$ can be given a physical interpretation. Thus, local fluctuations in density and size may be expressed in normalized form as

$$\delta\rho_0(\mathbf{r})=\frac{1}{\rho}\left(\sum_{j=1}^N\delta(\mathbf{r}-\mathbf{r}_j)-\rho\right), \tag{19}$$

$$\delta\rho_1(\mathbf{r})=\frac{1}{\bar{\sigma}\rho s_\sigma}\left(\sum_{j=1}^N\sigma_j\delta(\mathbf{r}-\mathbf{r}_j)-\bar{\sigma}\rho\right). \tag{20}$$

Their spatial correlations are then given by

$$\langle \delta\rho_0(\mathbf{r})\,\delta\rho_0(0)\rangle = \frac{\delta(\mathbf{r})}{\rho} + [g_{00}(r) - 1], \tag{21}$$

$$\langle \delta\rho_1(\mathbf{r})\,\delta\rho_0(0)\rangle = -g_{10}(r), \tag{22}$$

$$\langle \delta\rho_1(\mathbf{r})\,\delta\rho_1(0)\rangle = \frac{\delta(\mathbf{r})}{\rho} + g_{11}(r). \tag{23}$$

III. POTENTIAL MODELS WITHOUT AND WITH AN ATTRACTIVE WELL

Two familiar potentials are used here to model a polydisperse colloidal monolayer: (a) the repulsive part of the DLVO interaction[12–14] and (b) the Lennard-Jones 12-6 interaction.[15]

For charged hard spheres of polydisperse diameters σ, the repulsive DLVO potential, of Yukawa form, is

$$\beta\phi(r,\sigma_1,\sigma_2) = \begin{cases} \infty, & r < \sigma_{12} \\ A(\sigma_1)A(\sigma_2)\exp(-\kappa r)/r, & r > \sigma_{12} \end{cases}, \tag{24}$$

$$A(\sigma) = \frac{Z(\sigma) L_B^{1/2}\, \exp(\kappa\sigma/2)}{1 + \kappa\sigma/2},$$

where $\sigma_{12} \equiv (\sigma_1 + \sigma_2)/2$. In these expressions, κ is the inverse Debye-Hückel screening length determined by the counterion concentration and $L_B = e^2/4\pi\epsilon_0\epsilon k_B T$ the Bjerrum length. The charged mesospheres are assumed to have a constant surface charge density,[19] so that their resulting charge polydispersity is mapped onto the size polydispersity according to

$$Z(\sigma) = Z_{\bar{\sigma}} \left(\frac{\sigma}{\bar{\sigma}} \right)^2, \tag{25}$$

where $Z_{\bar{\sigma}}$ is the number of elementary charges on a particle of mean diameter $\bar{\sigma}$. We use the parameter values of Crocker and Grier:[4] $\bar{\sigma} = 650$ nm, $L_B = 0.715$ nm, $\kappa\bar{\sigma} = 4.0$, and $Z_{\bar{\sigma}} = 1990$. Under these conditions, electrostatic repulsion keeps the hard spheres from touching, so that only charge polydispersity is relevant in practice.

A closure relation proposed by Rogers and Young,[20]

$$g^{RY}(r,\sigma_1,\sigma_2) = e^{-\beta\phi(r,\sigma_1,\sigma_2)} \left\{ 1 + \frac{e^{m(r)\gamma(r,\sigma_1,\sigma_2)} - 1}{m(r)} \right\}, \tag{26}$$

has proven to be very successful for purely repulsive potentials such as (24). This equation mixes, via the function

$$m(r) = 1 - e^{-\lambda r}, \tag{27}$$

the Percus-Yevick and hypernetted-chain closures,[15] which separately bracket the exact results. The parameter λ in Eq. (27) is chosen to enforce consistency between the inverse compressibility calculated from Eq. (16) and that obtained by numerical differentiation of Eq. (15). We will use the RY closure below for the DLVO potential.

To model the effective attraction observed between colloidal spheres forming a monolayer between charged glass plates,[5,6] we use the simple Lennard-Jones potential,

$$\beta\phi(r,\sigma_1,\sigma_2) = 4\beta\epsilon \left[\left(\frac{\sigma_{12}}{r} \right)^{12} - \left(\frac{\sigma_{12}}{r} \right)^{6} \right], \tag{28}$$

where σ_{12} is defined as above. The Percus-Yevick and hypernetted-chain closures do not, in general, bracket the exact results for potentials with an attractive tail and so the RY closure is not as successful for such cases. Here we will use instead a different closure ''mix'' proposed by Zerah and Hansen,[21]

$$g^{ZH}(r,\sigma_1,\sigma_2) = e^{-\beta\phi_{sr}(r,\sigma_1,\sigma_2)} \times \left\{ 1 + \frac{e^{m(r)[-\beta\phi_{lr}(r,\sigma_1,\sigma_2) + \gamma(r,\sigma_1,\sigma_2)]} - 1}{m(r)} \right\}, \tag{29}$$

where $m(r)$ and its parameter λ are defined as in the RY closure. The ZH equation requires a separation of the potential $\phi = \phi_{sr} + \phi_{lr}$ into a repulsive short-range (sr) part and an attractive long-range (lr) part. We use for this the WCA scheme,[22]

$$\beta\phi_{sr}(r,\sigma_1,\sigma_2) = \begin{cases} \beta\phi(r,\sigma_1,\sigma_2) + \beta\epsilon, & r < r_{\min} \\ 0, & r > r_{\min} \end{cases},$$

$$\beta\phi_{lr}(r,\sigma_1,\sigma_2) = \begin{cases} -\beta\epsilon, & r < r_{\min} \\ \beta\phi(r,\sigma_1,\sigma_2), & r > r_{\min} \end{cases}, \tag{30}$$

where $r_{\min} \equiv 2^{1/6}\sigma_{12}$. The well depth is set at $\beta\epsilon = 0.25$, between $\beta\epsilon = 0.2$ found by Kepler and Fraden[5] and $\beta\epsilon \approx 0.3$ found by Carbajal *et al.*[6]

IV. RESULTS FOR THE SCHULZ DISTRIBUTION

The results presented in this section for two models of a monolayer of polydisperse colloidal spheres are based on the Schulz distribution[23] of sphere diameters σ. For particles with a mean diameter $\bar{\sigma}$, this is

$$f(\sigma) = \left(\frac{\alpha+1}{\bar{\sigma}} \right)^{\alpha+1} \frac{\sigma^\alpha e^{-(\alpha+1)\sigma/\bar{\sigma}}}{\Gamma(\alpha+1)}, \tag{31}$$

where $\Gamma(z)$ is the gamma function. The relative standard deviation of this distribution is

$$s_\sigma \equiv \frac{[\langle\sigma^2\rangle - \langle\sigma\rangle^2]^{1/2}}{\langle\sigma\rangle} = \frac{1}{(\alpha+1)^{1/2}}, \tag{32}$$

TABLE I. Computed thermodynamics of a polydisperse colloidal monolayer with repulsive DLVO potential and Schulz distribution of relative standard deviation s_σ.

$\rho\bar{\sigma}^2$	s_σ	$\beta U/N$	$\beta p/\rho$	$\rho k_B T K_T$
0.05	0	0.1336	1.729	0.3587
	0.1	0.1334	1.728	0.3587
	0.2	0.1329	1.727	0.3590
	0.3	0.1319	1.725	0.3593
0.10	0	0.4544	3.434	0.1168
	0.1	0.4540	3.435	0.1166
	0.2	0.4527	3.437	0.1163
	0.3	0.4504	3.442	0.1157
0.15	0	1.3030	7.742	0.0368
	0.1	1.3041	7.761	0.0366
	0.2	1.3065	7.811	0.0362
	0.3	1.3090	7.891	0.0354

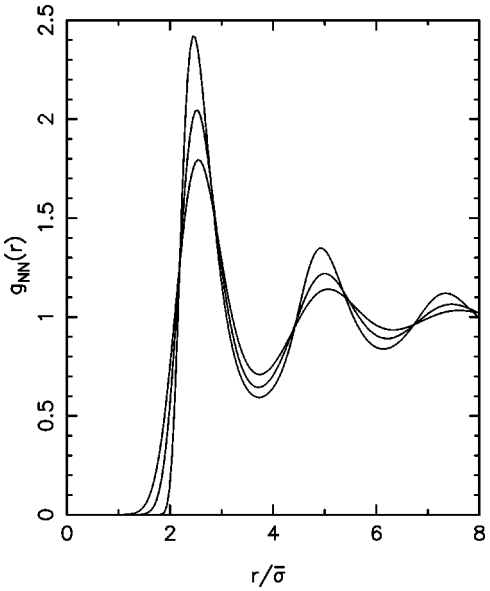

FIG. 1. The number-number pair distribution function $g_{NN}(r)=g_{00}(r)$ for a polydisperse colloidal monolayer with repulsive DLVO potential at density $\rho\overline{\sigma^2}=0.15$. The size dispersion of the colloidal spheres in descending order of the first peak is $s_\sigma=0$, 0.2, and 0.3.

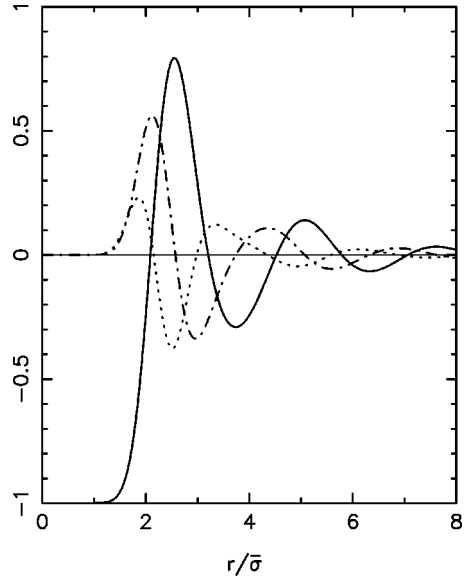

FIG. 3. Pair correlation function coefficients $g_{00}(r)-1$ (solid line), $g_{10}(r)$ (dash-dot line), and $g_{11}(r)$ (dotted line) for a polydisperse colloidal monolayer with repulsive DLVO potential at density $\rho\overline{\sigma^2}=0.15$ and size dispersion $s_\sigma=0.3$.

which will be used to characterize the suspensions and define the parameter α. The orthonormal polynomials satisfying Eq. (8) for the Schulz distribution $f(\sigma)$ are

$$p_j(\sigma)=\left[\frac{j!\Gamma(\alpha+1)}{\Gamma(j+\alpha+1)}\right]^{1/2} L_j^{(\alpha)}\left((\alpha+1)\frac{\sigma}{\bar{\sigma}}\right), \tag{33}$$

where the $L_j^{(\alpha)}(t)$ are the associated Laguerre polynomials.

We present first the results for the repulsive DLVO potential. Computed thermodynamic values are shown in Table I for $\rho\overline{\sigma^2}=0.05$, 0.10, 0.15 and three Schulz distributions of increasing width, $s_\sigma=0.1$, 0.2, 0.3, as well as the monodisperse case, $s_\sigma=0$, for reference. These quantities are seen to be relatively insensitive to the charge dispersion for the highly charged particles of the present sample. The effect of increasing polydispersity on the number-number distribution function $g_{NN}(r)$ is seen in Fig. 1 for $\rho\overline{\sigma^2}=0.15$. The general pattern of decreasing structure with increasing dispersion reproduces the behavior of polydisperse colloids in three dimensions.[19] This is further mirrored in the number-number structure factor $S_{NN}(k)$, shown in Fig. 2. (The g_{NN} and S_{NN} curves for $s_\sigma=0.1$ are quite close to their monodisperse limits and are omitted in Figs. 1 and 2 for clarity.) The functions $g_{00}(r)-1$, $g_{10}(r)$, and $g_{11}(r)$ for correlations of density-density, size-density, and size-size fluctuations, respectively, Eqs. (21)–(23), are shown in Fig. 3 for density $\rho\overline{\sigma^2}=0.15$ and dispersion $s_\sigma=0.3$. We see, for example, that at the first peak of $g_{00}(r)$, which occurs at $r=2.54\bar{\sigma}$, the size-size fluc-

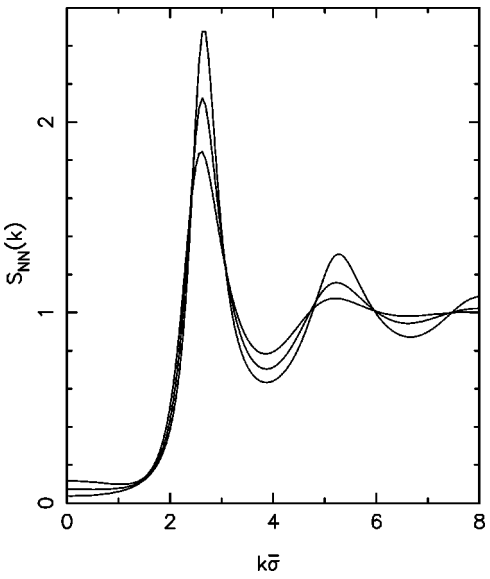

FIG. 2. The number-number structure factor $S_{NN}(k)=1+\rho\tilde{h}_{00}(k)$ for a polydisperse colloidal monolayer with repulsive DLVO potential at density $\rho\overline{\sigma^2}=0.15$. The size dispersion of the colloidal spheres in descending order of the first peak is $s_\sigma=0$, 0.2, and 0.3. The value at $k=0$ is largest for $s_\sigma=0.3$.

TABLE II. Computed thermodynamics of a polydisperse colloidal monolayer with Lennard-Jones potential of well depth $\beta\epsilon=0.25$ and Schulz distribution of relative standard deviation s_σ.

$\rho\overline{\sigma^2}$	s_σ	$\beta U/N$	$\beta p/\rho$	$\rho k_B T K_T$
0.2	0	−0.0882	1.232	0.6468
	0.1	−0.0887	1.234	0.6449
	0.2	−0.0901	1.239	0.6389
	0.3	−0.0926	1.247	0.6291
0.4	0	−0.1736	1.658	0.3459
	0.1	−0.1745	1.665	0.3426
	0.2	−0.1775	1.688	0.3328
	0.3	−0.1824	1.727	0.3168
0.6	0	−0.2383	2.541	0.1540
	0.1	−0.2389	2.568	0.1510
	0.2	−0.2408	2.651	0.1423
	0.3	−0.2431	2.801	0.1287

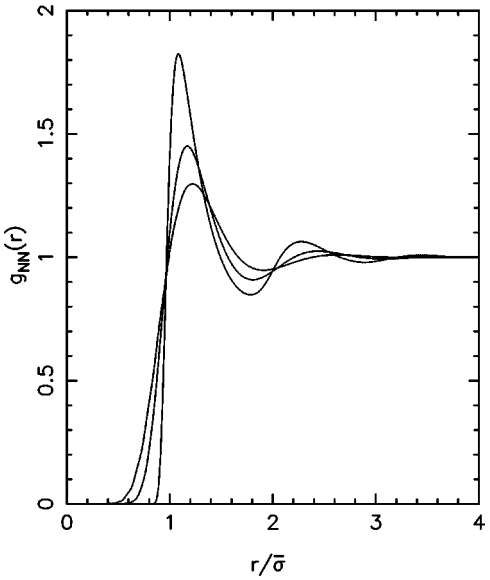

FIG. 4. The number-number pair distribution function $g_{NN}(r)=g_{00}(r)$ for a polydisperse colloidal monolayer with Lennard-Jones potential ($\beta\epsilon=0.38$) at density $\rho\bar{\sigma^2}=0.48$. The size dispersion of the colloidal spheres in descending order of the first peak is $s_\sigma=0$, 0.2, and 0.3.

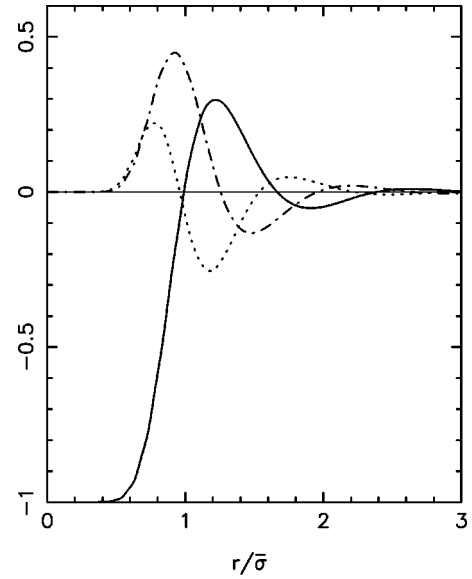

FIG. 6. Pair correlation function coefficients $g_{00}(r)-1$ (solid line), $g_{10}(r)$ (dash-dot line), and $g_{11}(r)$ (dotted line) for a polydisperse colloidal monolayer with Lennard-Jones potential ($\beta\epsilon=0.38$) at density $\rho\bar{\sigma^2}=0.48$ and size dispersion $s_\sigma=0.3$.

tuations are *negatively* correlated, while the cross correlation of size and density fluctuations passes through zero. This means that large spheres (large charges) are generally surrounded by small spheres (small charges) and vice versa.

Thermodynamic results for the polydisperse Lennard-Jones potential[24] for well depth $\beta\epsilon=0.25$ are gathered in Table II for three densities, $\rho\bar{\sigma^2}=0.2$, 0.4, 0.6, and the same four values of s_σ as above. Here the trends with increasing dispersion are consistent for the three densities—the internal energy becomes more negative, the pressure increases, and the compressibility decreases—in contrast to the mixed behavior seen for the purely repulsive potential in Table I; the percentage changes of these numbers with increasing s_σ are also several times larger than Table I data. The comparatively greater effect of the polydispersity is seen also in the g_{NN} and S_{NN} curves for the Lennard-Jones model, Figs. 4 and 5, compared to Figs. 1 and 2 for the repulsive DLVO potential, and further in the larger peaks of $g_{10}(r)$ and $g_{11}(r)$ relative to $g_{00}(r)-1$ in Fig. 6, compared to Fig. 3. The phenomenon of small spheres having large nearest neighbors and vice versa, seen again in Fig. 6 for $s_\sigma=0.3$, is shared with the other model.

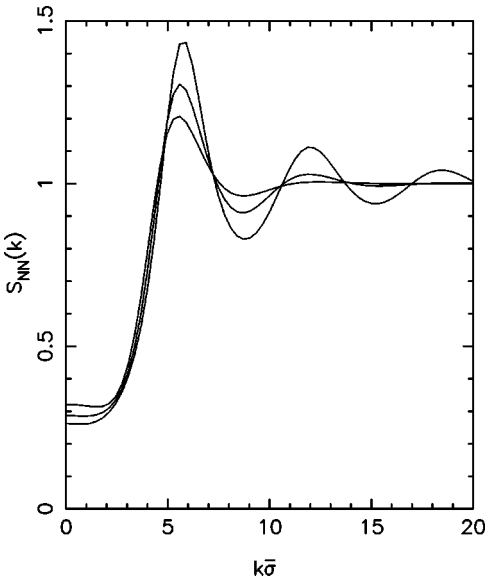

FIG. 5. The number-number structure factor $S_{NN}(k)=1+\rho\tilde{h}_{00}(k)$ for a polydisperse colloidal monolayer with Lennard-Jones potential ($\beta\epsilon=0.38$) at density $\rho\bar{\sigma^2}=0.48$. The size dispersion of the colloidal spheres in descending order of the first peak is $s_\sigma=0$, 0.2, and 0.3. The value at $k=0$ is largest for $s_\sigma=0.3$.

The model parameters for the curves displayed in Figs. 4–6, namely, a well depth $\beta\epsilon=0.38$ and a density $\rho\bar{\sigma^2}=0.48$, are chosen to approximate the highest density quasi-two-dimensional colloidal suspension reported by Carbajal *et al.*[6] These authors note that, for their larger plate separations, displacements of the colloidal spheres perpendicular to the midplane between the glass plates lead to changes in the observed structures (''dimensionality effects'') that in fact are similar to the effects of polydispersity seen in Figs. 1 and 4. (It is, of course, evident that the Schulz distribution is not an appropriate *quantitative* model of the effective polydispersity due to such perpendicular displacements.) In absolute terms, the curve for $s_\sigma=0$ in Fig. 4 shows a ''compressed'' structure compared to the measured $\rho\bar{\sigma^2}=0.48$ shape in Fig. 1(b) of Ref. 6, suggesting perhaps that the attractive well of the effective potential for the confined colloid has a shorter range than that of the Lennard-Jones potential.

ACKNOWLEDGMENTS

I thank the Dirección General de Investigación y Desarrollo (Spain) for sabbatical support under Grant No. SAB95-

0373. This work was supported in part by the Dirección General de Investigación Científica y Técnica (Spain) under Grant No. PB94-0112.

[1] S. Inoué, *Video Microscopy* (Plenum, New York, 1989).
[2] D. H. van Winkle and C. A. Murray, J. Chem. Phys. **89**, 3885 (1988).
[3] C. A. Murray, D. H. van Winkle, and R. A. Wenk, Phase Transitions **21**, 93 (1990).
[4] J. C. Crocker and D. G. Grier, Phys. Rev. Lett. **73**, 352 (1994).
[5] G. M. Kepler and S. Fraden, Phys. Rev. Lett. **73**, 356 (1994).
[6] M. D. Carbajal Tinoco, F. Castro Román, and J. L. Arauz Lara, Phys. Rev. E **53**, 3745 (1996).
[7] H. Löwen, J. Phys.: Condens. Matter **4**, 10105 (1992).
[8] H. Aranda Espinoza, M. Carbajal Tinoco, E. Urrutia Bañuelos, J. L. Arauz Lara, M. Medina Noyola, and J. Alejandre, J. Chem. Phys. **101**, 10925 (1994).
[9] B. Löhle and R. Klein, Physica A **235**, 224 (1997).
[10] H. Aranda Espinoza, M. Medina Noyola, and J. L. Arauz Lara, J. Chem. Phys. **99**, 5462 (1993).
[11] M. Chávez Páez, J. M. Méndez Alcaraz, J. L. Arauz Lara, and M. Medina Noyola, J. Colloid Interface Sci. **179**, 426 (1996).
[12] B. V. Derjaguin and L. D. Landau, Acta Physicochim. URSS **14**, 633 (1941).
[13] E. J. W. Verwey and J. T. G. Overbeek, *Theory of the Stability of Lyophobic Colloids* (Elsevier, Amsterdam, 1948).
[14] J. Israelachvili, *Intermolecular and Surface Forces*, 2nd ed. (Academic, New York, 1991).
[15] J.-P. Hansen and I. R. McDonald, *Theory of Simple Liquids* (Academic, London, 1986).
[16] F. Lado, Phys. Rev. E **54**, 4411 (1996).
[17] F. Lado, J. Chem. Phys. **49**, 3092 (1968); J. Comput. Phys. **8**, 417 (1971).
[18] B. D'Aguanno, R. Klein, J. M. Méndez Alcaraz, and G. Nägele, in *Complex Fluids*, edited by L. Garrido (Springer, Berlin, 1993).
[19] B. D'Aguanno and R. Klein, Phys. Rev. A **46**, 7652 (1992).
[20] F. J. Rogers and D. A. Young, Phys. Rev. A **30**, 999 (1984).
[21] G. Zerah and J.-P. Hansen, J. Chem. Phys. **84**, 2336 (1986).
[22] J. D. Weeks, D. Chandler, and H. C. Andersen, J. Chem. Phys. **54**, 5237 (1971).
[23] G. V. Schulz, Z. Phys. Chem. Abt. A **43**, 25 (1939).
[24] Extensive results for a monodisperse two-dimensional Lennard-Jones fluid in Percus-Yevick approximation have been given by E. D. Glandt and D. D. Fitts, J. Chem. Phys. **66**, 4503 (1977).